Chemosphere 171 (2017) 671–680

Contents lists available at ScienceDirect

Chemosphere

journal homepage: www.elsevier.com/locate/chemosphere

Fibrillar vs crystalline nanocellulose pulmonary epithelial cell responses: Cytotoxicity or inflammation?

Autumn L. Menas [a, 1], Naveena Yanamala [a, 1], Mariana T. Farcas [a], Maria Russo [c], Sherri Friend [b], Philip M. Fournier [d], Alexander Star [d], Ivo Iavicoli [e], Galina V. Shurin [f], Ulla B. Vogel [g], Bengt Fadeel [h], Donald Beezhold [i], Elena R. Kisin [a, 1], Anna A. Shvedova [a, j, *]

[a] Exposure Assessment Branch/NIOSH/CDC, Morgantown, WV, USA
[b] Pathology & Physiology Research Branch/NIOSH/CDC, Morgantown, WV, USA
[c] Institute of Public Health, Section of Occupational Medicine, Catholic University of the Sacred Heart, Rome, Italy
[d] Department of Chemistry, University of Pittsburgh, Pittsburgh, PA, USA
[e] Department of Public Health, Division of Occupational Medicine, University of Naples Federico II, Naples, Italy
[f] Department of Pathology, University of Pittsburgh Medical Center, Pittsburgh, PA, USA
[g] National Research Centre for the Working Environment, Copenhagen, Denmark
[h] Division of Molecular Toxicology, Institute of Environmental Medicine, Karolinska Institutet, Stockholm, Sweden
[i] Health Effects Laboratory Division/NIOSH/CDC, Morgantown, WV, USA
[j] Department of Physiology and Pharmacology, West Virginia University, Morgantown, WV, USA

HIGHLIGHTS

- Biological Responses of NC are orchestrated by their dimensions and morphology.
- NCF cytotoxicity may be caused by oxidative stress and not cellular uptake.
- Viability and oxidative damage models may not be effective in predicting toxicity.
- NC with different morphologies revealed drastic changes in the cytokine profiles.
- Exposure to various NC revealed distinct cytotoxic responses and cytokine signatures.

GRAPHICAL ABSTRACT

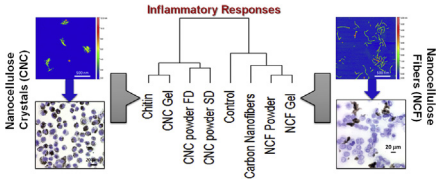

ARTICLE INFO

Article history:
Received 4 November 2016
Received in revised form
12 December 2016
Accepted 20 December 2016
Available online 24 December 2016

Handling Editor: A. Gies

Keywords:
Nanocellulose

ABSTRACT

Nanocellulose (NC) is emerging as a highly promising nanomaterial for a wide range of applications. Moreover, many types of NC are produced, each exhibiting a slightly different shape, size, and chemistry. The main objective of this study was to compare cytotoxic effects of cellulose nanocrystals (CNC) and nanofibrillated cellulose (NCF). The human lung epithelial cells (A549) were exposed for 24 h and 72 h to five different NC particles to determine how variations in properties contribute to cellular outcomes, including cytotoxicity, oxidative stress, and cytokine secretion. Our results showed that NCF were more toxic compared to CNC particles with respect to cytotoxicity and oxidative stress responses. However, exposure to CNC caused an inflammatory response with significantly elevated inflammatory cytokines/chemokines compared to NCF. Interestingly, cellulose staining indicated that CNC particles, but not NCF, were taken up by the cells. Furthermore, clustering analysis of the inflammatory cytokines revealed a

* Corresponding author. Exposure Assessment Branch (MS-2015), 1095 Willowdale Road, Morgantown, WV, 26505, USA.
E-mail address: ats1@cdc.gov (A.A. Shvedova).
[1] These authors have contributed equally.

http://dx.doi.org/10.1016/j.chemosphere.2016.12.105
0045-6535/Published by Elsevier Ltd.

Oxidative stress
Cytoxicity
Cytokine production
Lung epithelial cells

similarity of NCF to the carbon nanofibers response and CNC to the chitin, a known immune modulator and innate cell activator. Taken together, the present study has revealed distinct differences between fibrillar and crystalline nanocellulose and demonstrated that physicochemical properties of NC are critical in determining their toxicity.

Published by Elsevier Ltd.

1. Introduction

In recent years, considerable attention has been placed on the development of eco-friendly products for use in manufacturing industry. The unique properties of nano-scale materials have made them attractive for a number of innovative, sustainable, and green applications (Iavicoli et al., 2014). Nanocellulose (NC) is an emerging class of nanomaterials possessing unique physical/structural properties featuring low cost, renewable, biodegradable, and biocompatible products (Roman, 2015). NC has been employed for a number of potential applications in polymer nanocomposites, tissue engineering, drug delivery vehicles, artificial blood vessels constructs, and wound dressings (Österberg and Cranston, 2014). Nonetheless, the high aspect ratio and fibrous morphology of NC, coupled with its increased use in industry, raises safety concerns (Shvedova et al., 2014). Therefore, it is imperative to thoroughly assess toxicity of NC and health outcomes.

In general, toxicological testing of nanomaterials has proven to be challenging due to their many different sizes, shapes, coatings, and surface reactivity (Aillon et al., 2009; Farcal et al., 2015; Ivask et al., 2015). Furthermore, with respect to NC, differences in raw material sources (wood, algae, hemp or cotton), preparation procedures (acid hydrolysis or homogenization), and post-processing techniques (bleaching/autoclaving, spray/freeze drying) yield a wide range of NC with varied physicochemical properties. In the present study, a panel of CNC and NCF was investigated to determine whether differences in material features can lead to different cellular outcomes by employing lung cells as a cellular model system. CNC is a crystalline form of cellulose manufactured by acid hydrolysis providing long needle-like rods or “whiskers”. In contrast, NCF, produced via mechanical grinding and/or homogenization, forms long chains of soft fibrous structures.

Although many nanomaterials have been suggested to cause adverse health effects upon entering the body (Elsaesser and Howard, 2012; Landsiedel et al., 2012), current literature on the toxicity of NC is limited. Moreover, studies with conflicting results have provoked vastly different opinions on their safety and use. New and advanced cell culture-based approaches are gaining popularity in toxicology labs, driven by governmental and scientific demands (Perkel, 2012). Indeed, a number of *in vitro* exposure systems and lung specific bioassays have already been developed for the assessment of respiratory toxicity of airborne particles (Sayes et al., 2007). A study (Clift et al., 2011) applied a 3D *in vitro* triple cell co-culture model of the human epithelial airway showing cytotoxic responses accompanied by an increase in pro-inflammatory mediator release after exposure to CNC. There are some published studies on the genotoxicity of NCF in various cell models, with divergent outcomes (Catalan et al., 2015; de Lima et al., 2012). Furthermore, some *in vivo* studies have demonstrated evidence for NC toxicity. Another group (Cullen et al., 2000) found dose-dependent recruitment of inflammatory cells to the mouse peritoneal cavity after exposure to NCF. Similarly, we previously reported that exposure to respirable CNC causes oxidative stress, tissue damage, and inflammatory responses in mice following pharyngeal aspiration (Shvedova et al., 2016; Yanamala et al., 2014).

The thorough understanding of the biological behavior of nanomaterials is imperative for their safe use and future applications; however, for NC and its derivatives, such information is lacking and requires more attention. Increasing knowledge of the characteristics of nanomaterials that can be used to categorize them into hazard groups would aid greatly in risk assessment (Braakhuis et al., 2016). The aim of the current study was to compare five different NC particles using *in vitro* approaches to determine if certain characteristics (i.e. size, shape, origin) yield specific cytotoxicity effects. To this end, human lung alveolar epithelial cells (A549) were exposed to the different particles at three concentrations: 1.5 μg/cm^2, 15 μg/cm^2, and 45 μg/cm^2. Cell viability, levels of glutathione (GSH), release of cytokines/chemokines and transmission electron microscopy (TEM) imaging were employed to assess cellular effects following 24 h and 72 h of exposure. Cytokine profiles were compared to those induced by CNF and chitin, an abundant biopolymer with structural similarity to NC. Overall, these results indicate that size and shape of NC particles are critical in determining toxicity showing that CNC and NCF could induce distinctly different paradigm of toxic responses in lung cells.

2. Materials and methods

2.1. Particle preparation

Five different NC particles were employed for this study [CNC gel (10% wt.); CNC spray-dried powder (CNC SD); CNC freeze-dried powder (CNC FD); NCF gel (0.9% wt.); NCF freeze-dried powder (NCF powder)] to compare cytoxicity outcomes. All five NC particles were obtained from the USDA Forest Products Laboratory (Madison, WI). In addition, two other materials e.g. chitin and CNF were used as positive controls. Chitin derived from shrimp shells in a purified powder form was obtained from Sigma Aldrich (St. Louis, MO) and CNF was purchased from Pyrograf® Products, Inc. (Cedarville, OH). The particle characterization of CNF has been previously reported (Kisin et al., 2011). Stock solutions of each particle were first prepared in USP-grade sterile water at a concentration of ~3 mg/ml and were further diluted to 1 mg/ml prior to cell exposures. The particles were first sterilized by autoclaving followed by brief sonication (30 s) with a probe sonicator (Branson Sonifer 450, 10 W continuous output). Samples were also evaluated for bacterial endotoxin contamination, using a Peirce LAL Chromogenic Endotoxin Quantitation kit according to the manufacturer's instructions (Thermo Fisher Scientific, Grand Island, NY). Endotoxin levels for all used particles were below the detection limit (0.01 EU/ml) as determined by a Limulus amebocyte lysate (LAL) assay kit (Hycult Biotech, Inc., Plymouth Meeting, PA).

2.2. Particles characterization

Solutions of all particles were prepared by suspending the nanoparticles in USP grade sterile water. Atomic force microscopy

(AFM) samples were made by drop casting 5 μL of 20 mg/L solution on freshly cleaved mica. AFM was accomplished using a Multimode scanning probe microscope (Veeco) in tapping mode. An ACL probe (AppNano) was utilized at a frequency between 160 and 225 kHz, an amplitude set point between 1.5 and 1.8 V, and a drive amplitude between 100 and 300 mV. The resulting images were processed using Gwyddion (Brno, Czech Republic). Dynamic light scattering (DLS) analysis was performed on 1.0 g/L solutions using a Brookhaven Instrument Corporation ZetaPALS. A total of ten runs were averaged using 1.474 as the refractive index.

2.3. Cell culture and particle exposures

The human lung alveolar epithelial cell line A549 was obtained from the American Type Culture Collection (ATCC® CCL-185™). Cells were cultured in Dulbecco's Modified Eagle's Medium (DMEM) with 4.5 g/L Glucose (Lonza, Alpharetta, GA) supplemented with 10% fetal bovine serum (FBS, Atlanta Biologicals, Atlanta, GA), 1% L-glutamine (HyClone Life Technologies, Grand Island, NY), and 1% penicillin-streptomycin antibiotic (HyClone Life Technologies, Grand Island, NY) at 37 °C in a humidified atmosphere of 5% CO_2. Two exposure time-points (24 h and 72 h) and three concentrations of particles (1.5, 15 and 45 μg/cm^2) were employed to examine toxicity outcomes. Each condition (concentration and time point) was conducted in duplicate. A549 cell supernatants were collected after exposure and frozen at −80 °C until use for cytokine measurements. The cells were collected by treating with trypsin (Life Technologies, Grand Island, NY) followed by centrifugation at 800 rpm for 5 min (25 °C) and re-suspension in 1.0 ml PBS. The cells were used to measure cell viability, to perform TEM and staining. The remaining cells were frozen at −80 °C in order to lyse the cells and use for GSH and protein sulfhydryl (SH) analysis. The highest dose investigated (45 μg/cm^2) would result in 0.00073 μg of deposited dose per cell (~2 million cells per 96well-plate). A human equivalent workplace exposure to similar burden in alveolar type-II epithelial cells can be achieved in ~12 years (Erdely et al., 2013; NIOSH, 2010) at allowable exposure limits (5 mg/m^3 of cellulose) defined by Occupational Safety & Health Administration (OSHA). For further details on these calculations and the various parameters considered, please refer to the supplementary information section on the relevance of employed *in vitro* concentrations to realistic human exposures.

2.4. Transmission electron microscopy

TEM was employed to visualize A549 morphological changes 24 h and 72 h post exposure to different CNC and NCF materials. Cells were collected and fixed in 0.5–1.0 ml of Karnovsky's fixative (2.5% glutaraldehyde, 2.5% paraformaldehyde in 0.1 M Sodium Cacodylic buffer) and post-fixed in 2% osmium tetroxide for 1 h. The cells were then dehydrated and embedded in Epon, sectioned, and stained with Reynold's lead citrate and uranyl acetate. Micrographs of the cells were obtained on a JEOL TEM 1220 microscope (Peabody, MA) at a working voltage of 80 kV.

2.5. Cellulose staining of exposed A549 cells

Visualization of NC in cells was performed using specific staining method described previously (Knudsen et al., 2015). Briefly, exposed A549 cells were fixed to glass slides by incubating in −20 °C acetone for 10 min. Cells were then air dried to evaporate the acetone and stored at −20 °C. To stain the cellulose, endogenous peroxidase was first blocked with Ultravison Hydrogen Peroxide Block (Thermo scientific, Fremont, CA) for 10 min. After washing with PBS, nonspecific avidin binding was blocked by incubating in 30% rabbit normal serum with avidin from Avidin/Biotin Blocking kit (Vector Laboratories, Burlingame, CA) for 30 min and then removed by gentle suction. A biotinylated carbohydrate binding module (CBM) of β-1,4-glycanase (EXG:CBM) from the bacterium *Cellulomonas fimi* was then applied for 60 min. Slides were washed again with PBS, then streptavidin peroxidase conjugated (Rockland, Limerick, PA) was applied for 30 min. After washing with PBS a final time, peroxidase enzyme activity was visualized by incubation in Large Volume DAB Chromogen Single Solution (Thermo Scientific) to develop the staining for 5 min. The cells were then counterstained with Meyer's hematoxylin.

2.6. Cell viability assay

Cell viability was measured using a trypan blue exclusion staining method. After 24 h and 72 h exposure, 20 μl of cell suspension (as described above) was added to 20 μl Trypan blue (Life Technologies, Grand Island, NY) and then analyzed using a Countess automated cell counter (Invitrogen Life Technologies, Grand Island, NY). Three independent measurements (n = 3) were conducted to obtain the mean and standard error for each treatment group.

2.7. Protein concentrations

To determine total protein content in the A549 cell lysates and supernatants, a modified Bradford assay was performed according to the manufacturer's instructions (BioRad, Hercules, CA), with bovine serum albumin as the standard. The protein was measured as the OD at a wavelength of 595 nm. Data for the detection of thiols and cytokines was normalized using the obtained protein concentrations (mg/ml).

2.8. Detection of GSH and SH

Glutathione level in A549 cell lysates was determined using ThioGlo®3 (Covalent Associates Incorporated, Corvallis, OR), a maleimide reagent which produces highly florescent adducts upon its reaction with −SH groups. To measure GSH, 100 μl of ThioGlo was added to 100 μl diluted cell lysate (20 μl cells + 80 μl PBS). A total of five replicates (n = 5) from each cell lysate sample were analyzed to obtain the mean and standard error. After 30 min incubation in the dark, the fluorescence was measured using a Synergy H1 plate reader (BioTek, Winooski, VT) with an excitation of 378 nm and emission of 446 nm and gain of 100. To measure protein sulfhydryl (SH), 10 μl of sodium dodecyl sulfate (SDS) was added to each well/sample immediately following the GSH measurement. After 1 h incubation in the dark the fluorescence was measured again using the same conditions listed above.

2.9. Cytokines/chemokines analysis

Levels of 27 different cytokines and chemokines were assessed in the supernatants of A549 cells exposed to the various NC particles for 24 h and 72 h using a human cytokine group I panel Bio-Plex system (Bio-Rad, Hercules, CA). The cells were also exposed to chitin or CNF (1.5, 15, 45 μg/cm^2) for comparison. Exactly 50 μl of A549 supernatant was used for analysis of cytokines/chemokines. Bio-Plex Manager 6.1 software (Bio-Rad, Tokyo) was employed to estimate the concentration of each cytokine/chemokine/growth factors according to their representative standard curves. Four

replicates (n = 4) of each supernatant sample were used in the assay. Data are represented as mean values (pg/mg protein) ± SEM. The detection limit for each cytokine for this assay is in the range of 0.5–14.6 pg/ml.

2.10. Cluster analysis of cytokine data

In order to differentiate between CNC and NCF nanoparticles based on their cytokine responses in A549 cells, hierarchical cluster analysis was performed. The measured cytokine concentrations were first converted to fold change compared to their levels in control samples and were then log_2-transformed. Cytokines having measurement values below the detection limit were not used in the analysis. Hierarchical agglomerative (bottom up) clustering analysis using R (RCoreTeam, 2014) was applied to group control and the samples corresponding to different doses of CNC/NCF in exposed A549 cells based on their cytokine expression profiles induced at each post-exposure time point. A detailed cluster analysis of samples exposed to different CNC/NCF before and after removing missing cytokines measurements was performed using "Euclidean" distance similarity between the different samples and by employing ward. D2 linkage distance between the members of the clusters. By combining cytokine and sample clustering, heat maps were created with colors corresponding to the relative expression levels of the cytokines at each time point and concentration. The heat map and cluster of similar cytokines profiles and samples corresponding to various nanoparticles studied were produced with package heat map built for R version 3.1.3 (RCoreTeam, 2014).

2.11. Statistical analysis

GSH/SH and cytokine results were compared using One Way ANOVA, while Two Way ANOVA was used for comparing cell viability data. All pairwise multiple comparison procedures (Holm-Sidak method) was applied for all assessments. Results are presented as mean ± SEM. A p value cutoff of $\leq$0.05 was considered statistically significant in all cases.

3. Results

3.1. Characterization of nanocellulose particles

The structure, dimension, and dispersibility of the CNC and NCF particles were characterized and are presented in Table 1 and Fig. 1. DLS gives the hydrodynamic diameter, while AFM provides the length and width of the individual particles. Height and amplitude representative images reveal the presence of needle- or rod-like morphologies for all tested particles. The DLS effective diameter and AFM length measurements for all materials – excluding NCF powder FD - correlated well. Comparable dimensions were seen for all CNC and NCF particles; however, DLS analysis revealed that NCF powder had the largest hydrodynamic diameter followed by NFC gel > CNC powder FD > CNC gel > CNC powder SD. NCF powder also had the highest polydispersity index, demonstrating a broad size distribution (Table 1). The remaining particles (NCF gel, CNC powder FD, CNC powder SD, and CNC gel) had a polydispersity index between 0.1 and 0.4 indicating a moderate size distribution. Additionally, dimensions of chitin were determined using TEM imaging. Chitin exhibits a stacked plate nanostructure with individual plates approximately 1 nm thick and an average projection area of 25.3 ± 10.2 nm^2. The CNF diameters in the samples ranged from 60 to 150 nm and the length of the individual particles is approximately 30–100 μm (Kisin et al., 2011).

Table 1
Morphological characterizations of nanocellulose particles. The average size/distribution and particle morphology were determined using DLS/AFM measurements. The measurements are represented as mean ± SD. The reported values correspond to the mean of ten separate runs.

Particle Type	DLS		AFM	
	Diameter (nm)	Polydispersity	Length (nm)	Width (nm)
CNC powder FD	149.8 ± 2.6	0.344 ± 0.009	158 ± 97	54 ± 17
CNC powder SD	96.6 ± 0.9	0.279 ± 0.008	104 ± 44	47 ± 11
CNC gel	137.5 ± 1.2	0.238 ± 0.008	209 ± 136	37 ± 15
NCF powder	1904.3 ± 631.6	0.431 ± 0.074	142 ± 14	28 ± 11
NCF gel	214.2 ± 6.2	0.400 ± 0.010	n/a	20 ± 4

3.2. Comparative cytotoxicity of different NC

The cytotoxic potential of CNC and NCF particles on A549 cells was determined using vital dye exclusion (Trypan blue) after 24 h and 72 h exposure. The viability after exposure to the three CNC materials followed the same general trend: all doses showed approximately 10–20% decrease in viability compared to respective controls at both time-points with no significant dose-dependent responses (Fig. 2). This was contrasted by the two NCF materials which exhibited a more significant decrease in cell viability and clear time-dependent responses. The viability was significantly lower at 72 h compared to 24 h for both NCF powder and NCF gel at all doses - except for the NCF powder 1.5 μg/cm^2 (Fig. 2B). Generally, a 40–50% decrease in viability was noted after NCF powder and gel exposure for 72 h, while only a 10–20% decrease was shown for 24 h of exposure. For comparison, CNF showed clear dose-dependent responses at both time-points, with the highest dose causing a decrease in viability of 70% compared to control (Fig. 2). Chitin, however, did not show a significant decrease in cell viability of A549 cells at any of the doses nor any time-dependent responses (Fig. 2).

3.3. Cellular morphology changes and cellular uptake of NC

TEM was employed to visualize A549 cells after exposure to the highest dose (45 μg/cm^2) of CNC and NCF particles. Morphological changes were seen starting at 24 h exposure with all CNC/CNF particles showing the presence of tonofilaments (dark pigment/elongated), vacuoles and lipid droplets formation (Fig. S1). At the 72 h exposure time point, a higher prevalence of lipid droplets, vacuoles and tonofilaments are present in the A549 cells, particularly in cells exposed to NCF powder, NCF gel and CNC powder (Fig. S2). A549 cells exposed to chitin and carbon nanofibers also show the presence of lipid droplets, vacuoles, and tonofilaments at both time points (Figs. S1G-H and S2G-H). Additionally, CNF nanoparticles can be clearly seen inside the cells (Figs. S1G and S2G).

Specific cellulose staining was used to visualize the presence/uptake of cellulose nanoparticles in A549 cells after 72 h exposure (Fig. 3). Interestingly, no nanoparticle uptake was seen for fibrous nanocellulose i.e., NCF materials were seen outside, mostly localized at the cell boundaries of A549 cells (Fig. 3, NCF Powder and Gel). However, CNC powder FD, CNC SD and CNC Gel can be clearly seen inside the cells, suggesting their uptake by A549 cells (Fig. 3, insets).

3.4. Oxidative stress responses upon exposure to NC

The extent of oxidative damage caused by CNC and NCF was determined by assessing GSH and SH levels in A549 cells exposed for 24 h and 72 h (Fig. 4). The same general trend in GSH levels

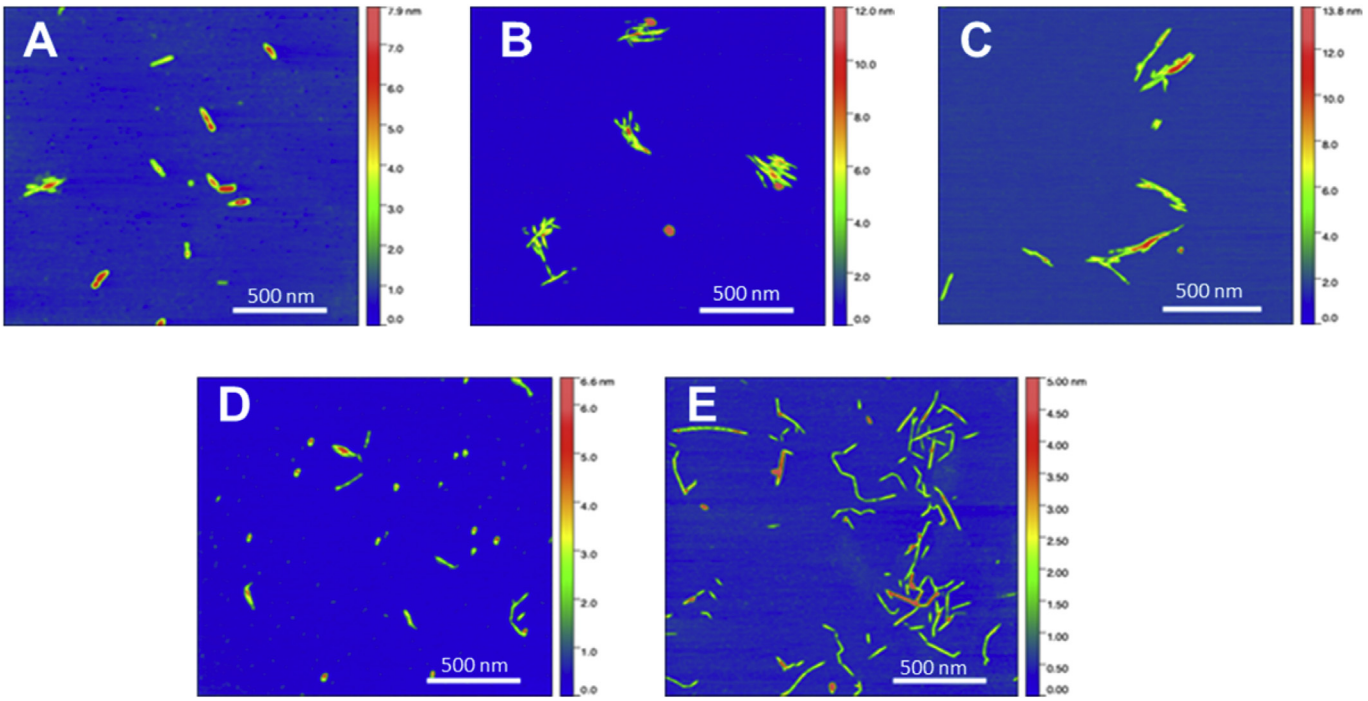

Fig. 1. Representative AFM images of nanocellulose particles where A – CNC Powder FD, B – CNC Powder SD, C – CNC Gel, D – NCF Powder, E – NCF Gel. Atomic force microscopy samples were made by drop casting 5 μL of 20 mg/L solution on freshly cleaved mica. AFM was accomplished using a Multimode scanning probe microscope (Veeco) in tapping mode. The resulting images were processed using Gwyddion (Brno, Czech Republic).

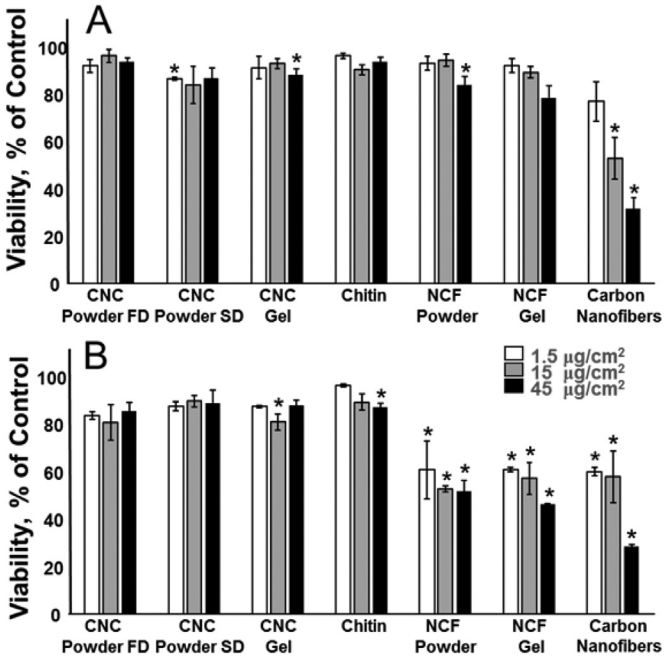

Fig. 2. A549 cell viability responses after 24 h (A) and 72 h (B) exposure. Cell viability was assessed by trypan blue exclusion assay. White columns represent cell viability after exposure with 1.5 μg/cm^2 of nanoparticles, grey columns – 15 μg/cm^2 and black columns – 45 μg/cm^2. The results are expressed as mean ± SEM. Significance shown as $p < 0.05$ compared to control (*) of two separate experiments ($n = 3$).

among the three concentrations of all tested nanoparticles was seen at both time-points, with lower levels of GSH detected at 72 h as compared to 24 h (Fig. 4A–B). Excluding CNC gel, all concentrations of CNC and NCF led to significantly lower levels of GSH compared to control at both time-points. Only NCF materials showed dose-dependent decrease in GSH levels at 24 h (Fig. 4A), while at 72 h NCF, as well as CNC powder (FD and SD), showed dose-dependent decreases in GSH levels (Fig. 4B). NCF caused a more pronounced decrease in GSH compared to CNC at both of the tested time-points. NCF and chitin displayed a clear dose-dependent effect (Fig. 4A) and the effect of chitin was more pronounced at 72 h compared to 24 h (Fig. 4B). Similar to GSH results, SH levels were not significantly altered after exposure to CNC gel at 24 h or 72 h (Fig. 4C–D). There was also no difference in levels of SH after exposure to CNC powder SD at 24 h (Fig. 4C). NCF powder and gel induced significantly decreased levels of SH compared to control and to CNC-based NPs. Moreover, dose-dependent decreases in SH levels occurred after exposure to NCF powder and gel at both time-points (Fig. 4C–D). CNF and chitin also triggered a decrease of SH, however, only CNF induced a dose-dependent reduction (Fig. 4C–D).

3.5. Secretion of cytokines, chemokines and growth factors

Cytokines and chemokines are important mediators of inflammatory responses. Therefore, 27 different cytokines/chemokines were measured in the supernatants of A549 cells exposed to NC particles for 24 h (Table S1) and 72 h (Table S2). For comparison, cells were also exposed to chitin and CNF. Interestingly, at both time points, cytokine levels were more elevated after exposure to CNC compared to NCF powder. In particular, CNC exposure (45 μg/cm^2) for 72 h significantly increased secretion of pro-inflammatory cytokines such as IL-6, IL-8, MCP-1, IL-1ra, IL-12p70 and G-CSF (Fig. 5). In contrast, NCF powder and gel induced decreased cytokine responses. Moreover, changes in most of the cytokines were time dependent for all particles. Notably, cells exposed to CNC or chitin secreted cytokines with a similar pattern (increasing with exposure time) while NCF-induced responses were found to be similar to CNF (stronger at 24 h).

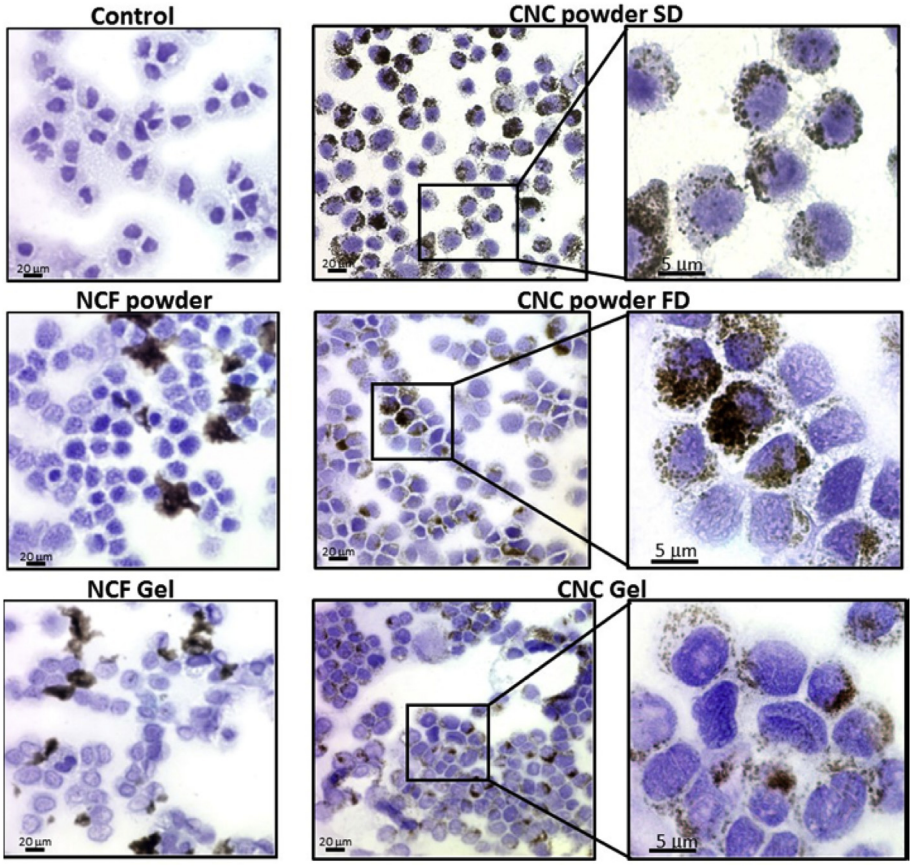

Fig. 3. Visualization of nanocellulose in A549 cells. Cellulose staining in A549 cells exposed to 45 μg/cm^2 of NC particles for 72 h was performed using a biotinylated carbohydrate binding module of β-1,4-glycanase. Nanocellulose uptake by A549 cells was found only after exposure to CNC powder FD, CNC powder SD and CNC Gel. No nanoparticle uptake was seen for fibrous nanocellulose: NCF powder and NCF gel.

3.6. Hierarchical cluster analysis of cytokine responses

In order to identify and differentiate responses of CNC and NCF particles, hierarchical cluster analysis was performed employing all the cytokine response data corresponding to the various concentrations tested for each particle. The results corresponding to the ward. D2 clustering method at 24 h and 72 h exposure are represented as a heat-map in Fig. 6 and S3. The heat map clearly shows areas of relatively high (green color) and low (red color) cytokine levels in certain clusters of samples. Notably, at the 24 h time-point (Fig. 6A), all concentrations of chitin and CNC Powder FD samples – with the exception of the 1.5 μg/cm^2 of CNC Powder FD, were clustered together with control or unexposed samples. While all concentrations corresponding to CNC gel, CNC powder SD and CNF samples with the exception of 1.5 μg/cm^2 concentration of CNF were clustered together, all concentrations of NCF gel and powder samples, with the exception of the 15 μg/cm^2 concentration of NCF gel formed a separate cluster suggesting a differential pattern of cytokine profiles compared to control as well as CNC samples (Fig. 6A). Furthermore, at 72 h of exposure, two major clusters separating CNC and NCF particles were observed, further suggesting a clear demarcation between fibrous versus crystalline (whisker) cellulose particles. As seen in Fig. 6B, all samples of CNC materials at all concentrations were clustered together with chitin, while NCF based materials were found to be segregated with CNF. Moreover, the close clustering between CNC powder FD and SD as well as CNC gel and chitin and the branching of various concentrations within each sub-cluster clearly suggests that these cellulose particles can be unequivocally separated based on the cytokine data. Overall, these results indicate that crystalline nanocellulose induces an inflammatory response, while fibrillar nanocellulose causes cytotoxicity in A549 cells. Moreover, morphological differences and similarities in cellulose based nanoparticles could be determined based on their cytokine responses.

4. Discussion

In the last decade there has been an increased interest towards “green” bio-based nanomaterials. NC originates from cellulose, the most abundant organic polymer on earth, and is therefore considered natural, renewable, biodegradable and biocompatible. NC materials have received a great deal of attention due to their outstanding properties, including low-density, high surface area, hydrophilicity, and increased tensile strength, stiffness, and strain, compared to other nanomaterials (Chinga-Carrasco and Syverud, 2012; Kalia et al., 2011; Moon et al., 2011; Peng et al., 2011). The same properties that make them excellent materials, however, may also have implications on their safety and use. NC may have diverse structural and chemical properties dependent on starting material and manufacturing process (e.g. freeze-dried *verses* spray-dried) (Peng et al., 2013). This needs to be considered as it is well established that nanoparticle size, shape, and morphology may influence toxicity (Hanif et al., 2014). Currently, no published results have revealed definite safety concerns of NC in the workplace, but indications of dose-dependent toxicity and inflammatory effects have

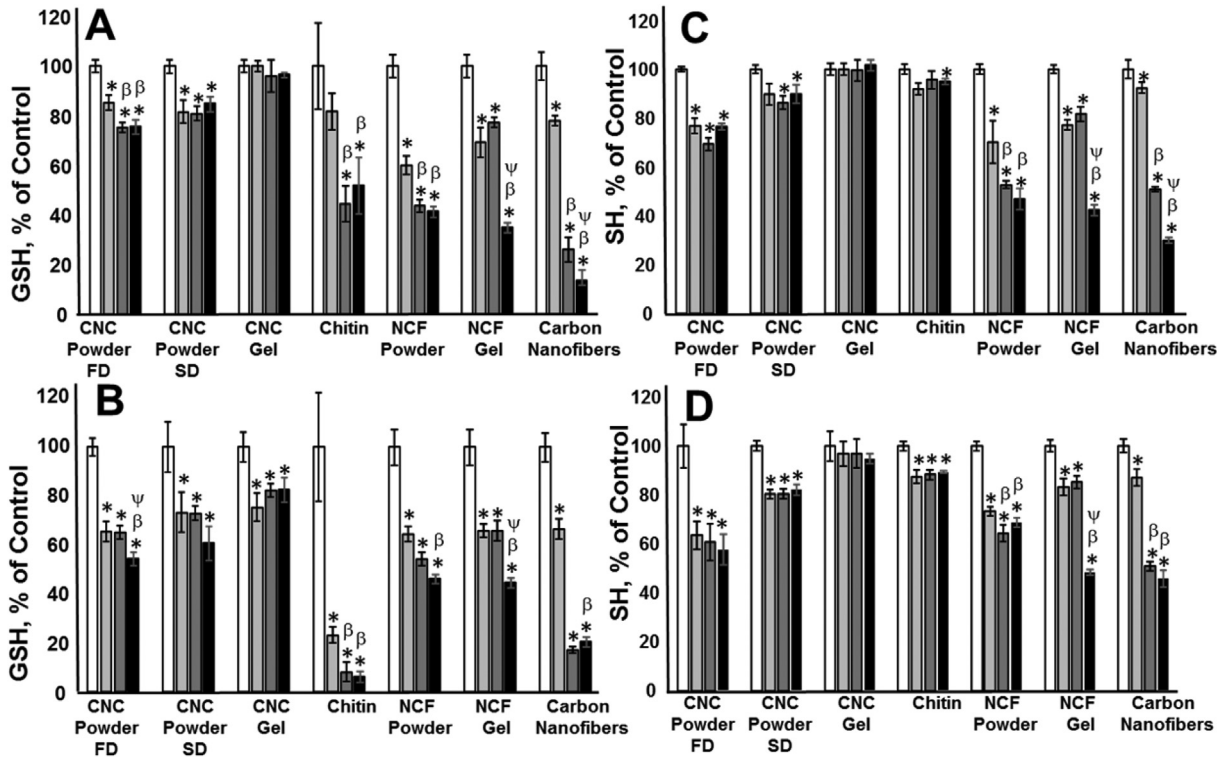

Fig. 4. Oxidative stress responses upon exposure to NC. Glutathione (GSH) and total thiol (SH) levels were evaluated in A549 cells exposed for 24 h (A, C) and 72hr (B,D) with three doses of different materials: white columns - control cell, light grey columns – 1.5 μg/cm^2 of nanoparticles, dark grey columns – 15 μg/cm^2 and black columns – 45 μg/cm^2. The results are expressed as mean ± SEM. Significance shown as $p < 0.05$ compared to control (*), to 5 μg/ml ($^{\beta}$), and to 50 μg/ml ($^{\Psi}$) of two separate experiments with $n = 5$.

been reported (Ni et al., 2012; Pereira et al., 2013). Therefore, it is imperative to thoroughly assess and understand the impact of NC on human health and the environment. Moreover, with the rapid increase in the number and diversity of NC materials generated from various sources and through different technological processes, alternative test strategies are required to reduce the reliance on primary animal testing. Thus the objective of the current study was to utilize such approaches to compare various types of NC materials to determine if biological responses of various NC materials is orchestrated by their differences in size, shape and morphology. This study compared two morphologically distinct NC particles (e.g., CNC and NCF) along with different post-processing method for each type. A549 cells were exposed to three different concentrations (1.5, 15 and 45 μg/cm^2) of five types of NC materials (three CNC and two NCF) and two well-characterized positive controls (CNF and chitin). Overall, our results indicate that various types of NC induce distinct cytotoxic responses and/or cytokine signatures in lung epithelial cells. Such studies would enable the selection of priority NC materials (e.g., highest toxicity within each category) to go forward with more focused mechanistic and/or targeted animal studies.

One of the most important findings of our study was the different cell viability and oxidative stress responses seen after exposure to CNC compared to NCF materials. Applying a standard "cut-off" - limit of 20–30% generally employed in toxicity modeling approaches, our study would imply that CNC materials are non-toxic to lung epithelial cells (Fig. 2). NCF materials, in contrast, caused a significant decrease in cell viability - with the lowest viability seen at the 72 h of exposure time-point (Fig. 2B). The decrease in GSH levels - considered a marker of oxidative stress - was similar to differences seen in cell viability, with the most significant decreases after exposure to NCF materials. Some dose-dependent decreases in GSH levels was also noted after CNC exposure; however, these changes were negligible compared to NCF exposure. Overall, the observed cytotoxicity of CNC and NCF materials in A549 cells were strongly correlated with oxidative stress responses.

Also, it is important to mention that the cellular uptake and inflammatory responses following exposure to CNC and NCF materials were quite different in A549 cells. Despite low cytotoxicity based on the cellular viability, CNC particles induced a more robust inflammatory response compared to NCF. A marked increase in various pro- and anti-inflammatory cytokines was found upon exposure to CNC materials (Tables S1 and S2, Fig. 5), similar to those responses seen in mice after pharyngeal aspiration with CNC (Yanamala et al., 2014). Most of the cytokine responses followed the same trend at both time-points of exposure. To better understand if these cytokine responses could be used to delineate the differences in toxicity induced by various forms and types of NC, clustering analysis was performed (Fig. 6). The results of the hierarchical clustering analysis identified distinct clusters separating the different types of NC materials based on their similarity in cytokine responses. Interestingly, discrete differences in cytokine responses were also noted between powder and gel forms of each NC type investigated. This indicates that even slight changes in production of NC materials could result in distinct cellular responses. Moreover, the inflammatory cytokine/chemokine levels in particular upon exposure to different CNC materials followed similar trends compared to their effective particle sizes i.e., CNC powder FD > CNC Gel ≥ CNC powder SD (Fig. 3, Table 1). Overall, we found that CNC is most similar to chitin while NCF responses were mostly parallel to CNF. It has been previously reported that chitin induces robust innate immune responses (Gandhi and Vliagoftis, 2015), while CNF are known to be cytotoxic and genotoxic (Kisin et al., 2011; Murray

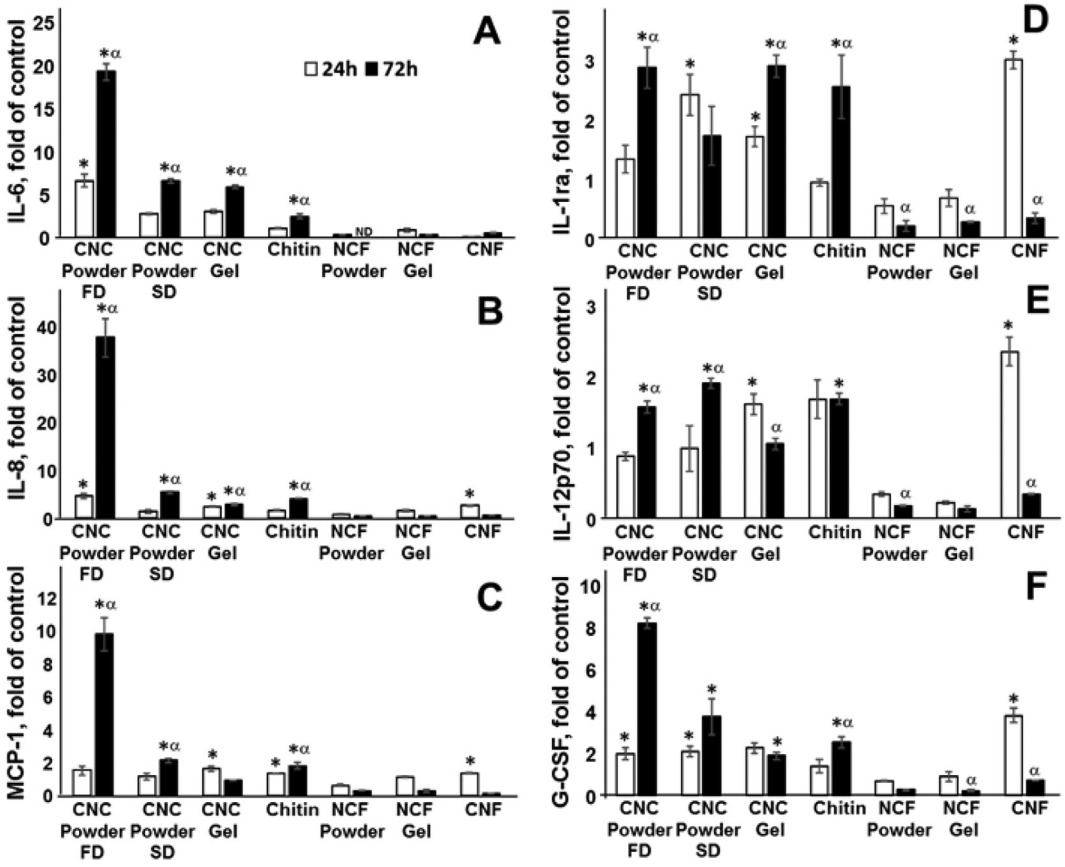

Fig. 5. Cytokine response induced by exposure to nanocellulose (45 μg/cm^2) for 24 h (white columns) and 72 h (black columns): A – IL-6, B – IL-8, C – MCP-1, D – IL-1ra, E – IL-12p70, F – G-CSF. These measurements were performed using Bio-Rad 27-plex human assay kit, composed of a combination of pro- and anti-inflammatory cytokines with a subset of chemokine's. The results are presented as mean ± SEM of 2 independent experiments in duplicates with n = 4 for each sample. Significance shown as $p < 0.05$ compared to control (*) and to 24 h exposure (α).

et al., 2012). Importantly, it has been reported that exposure to chitin can result in innate allergic inflammation characterized by alternatively activated macrophages and eosinophilia *in vivo* (Kogiso et al., 2011; Reese et al., 2007; Van Dyken et al., 2011). Chitin exposure is also correlated with asthma and other allergic diseases in humans (Van Dyken et al., 2011). However, exposure to chitin did not induce cytotoxicity in A549 cells, but triggered a robust inflammatory responses in this study. Similar to chitin, CNC also caused an increase in several factors including MCP-1/CCL-2, required for chitin-induced M2 polarization *in vivo* (Roy et al., 2012) and IL-8, a soluble mediator that plays an important role in airway remodeling (Hong et al., 2010; Pascual and Peters, 2005). This suggests that it becomes crucial to consider structural properties of nanomaterials and their resemblance to other biomolecules. Taken together these results supports the notion that both size and shape/structure plays a critical role in determining the biological responses of cellulose nanoparticles and their interactions with the cells. This is further supported by the studied uptake using cellulose immunostaining of A549 cells exposed to CNC or NCF (Fig. 3). The CNC materials with low cytotoxicity (Fig. 2), were taken up by A549 cells and induced a marked inflammatory response. However, no uptake was seen for fibrous nanocellulose i.e., NCF materials (Fig. 3), which exhibited cytotoxicity and increased oxidative stress in A549 cells (Figs. 2 and 6). This finding is surprising when one considers that the cytotoxicity of nanoparticles, in most cases, is correlated with cellular uptake. This suggests that the cytotoxicity of NCF materials in A549 cells may be caused by oxidative stress and not cellular uptake. However, the robust inflammatory responses found in the case of CNC particles could be a result of their active uptake by A549 cells. Taken together this study reveals that CNC and NCF particles may induce distinct responses in A549 cells through different mechanisms. While exposure to CNC particles triggered robust inflammatory responses, NCF particles – with larger diameter and smaller width's than CNC particles (Table 1) – induced cytotoxicity via oxidative stress mechanisms in A549 cells. Further studies aimed at defining and exploring the functional interactions of CNC and NCF materials with various cell types are needed to validate these findings.

5. Conclusions

The current study highlights the fact that using cellular models based on viability and oxidative damage responses alone may not be efficient in predicting the toxicity of cellulose nanoparticles. In particular, CNC particles were seemingly non-toxic and the different types of CNC tested (FD, SD and gel) could not be differentiated solely based on the viability and oxidative stress. However, comparative analysis of NC having different morphologies revealed drastic changes in the cytokine profiles despite low or no cytotoxicity. Also cellulose staining of exposed A549 cells indicated the uptake of CNC particles, but not NCF. Interestingly, effects of CNC were found to be akin to chitin while NCF were more similar to CNF outcomes, based on the cytokine profiles. Overall, the current work provides support for the notion that size and shape properties of NC materials are critical in determining toxicity that could further suggests inferred different mode of actions. Additional studies

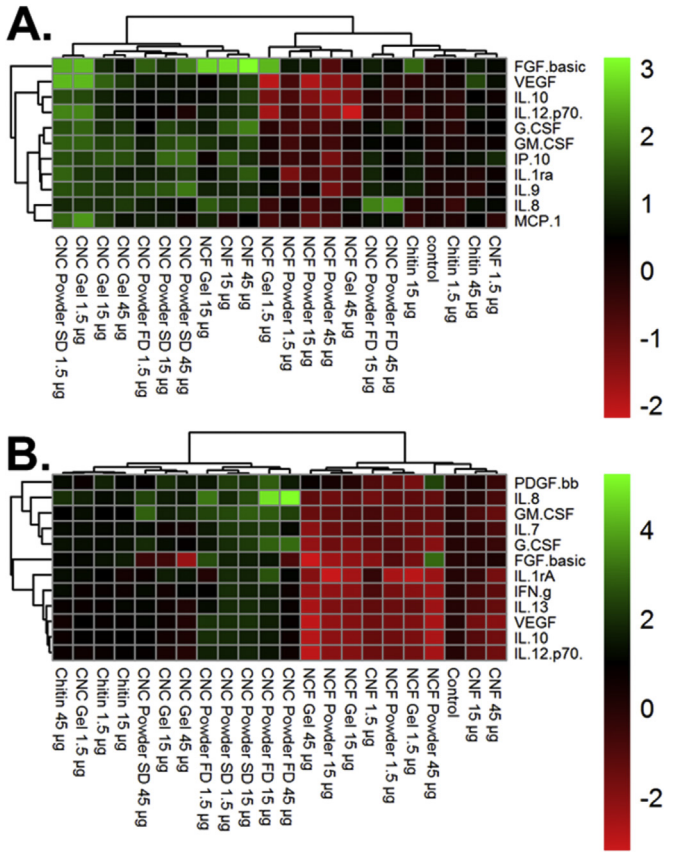

Fig. 6. Hierarchical cluster analysis of cytokine profiles in A549 cells exposed to various crystalline nanocellulose (CNC) and nanocellulose fiber (NCF) materials. The samples of A549 cells exposed to different concentrations of CNC and NCF along with respective controls (chitin and CNF) were clustered based on the Euclidean distance metric and ward. D2 clustering method at (A) 24 h and (B) 72 h post exposure time points. The samples corresponding to different nanoparticles and several cytokines measured (after removing missing values) in supernatants from each post exposure time point were also reordered based on their (dis-)similarities according to the dendrogram on the top and left, respectively. Each branch in the dendrogram shows the similarity between samples, i.e., the shorter the branch, the more similar. The heat map colors represent log2 transformed fold change values of cytokines relative to the minimum and maximum of all values, increasing from red to green, in each case. A key showing the range of values at each post exposure time point is also shown in the figure. (For interpretation of the references to colour in this figure legend, the reader is referred to the web version of this article.)

focusing on the underlying mechanisms including cellular interactions and recognition by specific receptors are underway to explore how different types of NC induce inflammation and cytotoxicity in cells. This study continues to point out the importance of considering various target endpoints, mechanisms or biological outcomes, not just classical assays (e.g., cytotoxicity), when evaluating the safety of nanomaterials using alternative test strategies. The findings presented in this study are limited to the type of nanocellulose based particles, cells and conditions investigated, and great care should be taken when generalizing our findings to other CNC and CNF types, isolated from different sources and those employing different extraction and fabrication methods. More studies that evaluate the mechanistic details of CNC and NCF interactions with cells employing sophisticated *in vitro* (e.g., 3D co-culture models) or ex vivo models that consider multiple target organ-specific cell types (Clift et al., 2011; Endes et al., 2014; 2015) and those that mimic *in vivo* like exposure conditions (e.g., pulmonary surfactant interactions) are still required to assess the potential health effects of CNC and NCF exposures and for understanding their toxicological profiles.

Disclaimer

The findings and conclusions in this report are those of the authors and do not necessarily represent the views of the National Institute for Occupational Safety and Health. Mention of trade names or commercial products does not constitute endorsement or recommendation for use. The authors declare no competing financial interest.

Acknowledgments

This work was supported by NTRC 939011K, NIH R01ES019304, NIOSH OH008282, and the European Commission (FP7-NANOSOLUTIONS, grant agreement no. 309329). The authors also want to thank Diane Schwegler-Berry for TEMs preparation, C. Højgaard, J.R. Winther, and M. Willemoës for providing the Biotinylated Carbohydrate Binding Module of β-1,4-Glycanase for visualization of nanocellulose.

Appendix A. Supplementary data

Supplementary data related to this article can be found at http://dx.doi.org/10.1016/j.chemosphere.2016.12.105.

References

Aillon, K.L., Xie, Y., El-Gendy, N., Berkland, C.J., Forrest, M.L., 2009. Effects of nanomaterial physicochemical properties on in vivo toxicity. Adv. Drug Deliv. Rev. 61 (6), 457–466.
Braakhuis, H.M., Oomen, A.G., Cassee, F.R., 2016. Grouping nanomaterials to predict their potential to induce pulmonary inflammation. Toxicol. Appl. Pharmacol. 2993–2997.
Catalan, J., Ilves, M., Jarventaus, H., Hannukainen, K.S., Kontturi, E., Vanhala, E., Alenius, H., Savolainen, K.M., Norppa, H., 2015. Genotoxic and immunotoxic effects of cellulose nanocrystals in vitro. Environ. Mol. Mutagen 56 (2), 171–182.
Chinga-Carrasco, G., Syverud, K., 2012. On the structure and oxygen transmission rate of biodegradable cellulose nanobarriers. Nanoscale Res. Lett. 7.
Clift, M.J., Foster, E.J., Vanhecke, D., Studer, D., Wick, P., Gehr, P., Rothen-Rutishauser, B., Weder, C., 2011. Investigating the interaction of cellulose nanofibers derived from cotton with a sophisticated 3D human lung cell coculture. Biomacromolecules 12 (10), 3666–3673.
Cullen, R.T., Searl, A., Miller, B.G., Davis, J.M., Jones, A.D., 2000. Pulmonary and intraperitoneal inflammation induced by cellulose fibres. J. Appl. Toxicol. 20 (1), 49–60.
de Lima, R., Oliveira Feitosa, L., Rodrigues Maruyama, C., Abreu Barga, M., Yamawaki, P.C., Vieira, I.J., Teixeira, E.M., Correa, A.C., Caparelli Mattoso, L.H., Fernandes Fraceto, L., 2012. Evaluation of the genotoxicity of cellulose nanofibers. Int. J. Nanomedicine 73555–73565.
Elsaesser, A., Howard, C.V., 2012. Toxicology of nanoparticles. Adv. Drug Deliv. Rev. 64 (2), 129–137.
Endes, C., Schmid, O., Kinnear, C., Mueller, S., Camarero-Espinosa, S., Vanhecke, D., Foster, E.J., Petri-Fink, A., Rothen-Rutishauser, B., Weder, C., Clift, M.J., 2014. An in vitro testing strategy towards mimicking the inhalation of high aspect ratio nanoparticles. Part Fibre Toxicol. 1140.
Endes, C., Mueller, S., Kinnear, C., Vanhecke, D., Foster, E.J., Petri-Fink, A., Weder, C., Clift, M.J., Rothen-Rutishauser, B., 2015. Fate of cellulose nanocrystal aerosols deposited on the lung cell surface in vitro. Biomacromolecules 16 (4), 1267–1275.
Erdely, A., Dahm, M., Chen, B.T., Zeidler-Erdely, P.C., Fernback, J.E., Birch, M.E., Evans, D.E., Kashon, M.L., Deddens, J.A., Hulderman, T., Bilgesu, S.A., Battelli, L., Schwegler-Berry, D., Leonard, H.D., McKinney, W., Frazer, D.G., Antonini, J.M., Porter, D.W., Castranova, V., Schubauer-Berigan, M.K., 2013. Carbon nanotube dosimetry: from workplace exposure assessment to inhalation toxicology. Part Fibre Toxicol. 10 (1), 53.
Farcal, L., Torres Andon, F., Di Cristo, L., Rotoli, B.M., Bussolati, O., Bergamaschi, E., Mech, A., Hartmann, N.B., Rasmussen, K., Riego-Sintes, J., Ponti, J., Kinsner-Ovaskainen, A., Rossi, F., Oomen, A., Bos, P., Chen, R., Bai, R., Chen, C., Rocks, L., Fulton, N., Ross, B., Hutchison, G., Tran, L., Mues, S., Ossig, R., Schnekenburger, J., Campagnolo, L., Vecchione, L., Pietroiusti, A., Fadeel, B., 2015. Comprehensive in vitro toxicity testing of a panel of representative oxide nanomaterials: first steps towards an intelligent testing strategy. PLoS One 10 (5), e0127174.
Gandhi, V.D., Vliagoftis, H., 2015. Airway epithelium interactions with aeroallergens: role of secreted cytokines and chemokines in innate immunity. Front. Immunol. 6147.
Hanif, Z., Ahmed, F.R., Shin, S.W., Kim, Y.K., Um, S.H., 2014. Size- and dose-dependent toxicity of cellulose nanocrystals (CNC) on human fibroblasts and colon adenocarcinoma. Colloids Surf. B Biointerfaces 119162–119165.

Hong, J.Y., Lee, K.E., Kim, K.W., Sohn, M.H., Kim, K.E., 2010. Chitinase induce the release of IL-8 in human airway epithelial cells, via Ca2+-dependent PKC and ERK pathways. Scand. J. Immunol. 72 (1), 15–21.
Iavicoli, I., Leso, V., Ricciardi, W., Hodson, L.L., Hoover, M.D., 2014. Opportunities and challenges of nanotechnology in the green economy. Environ. Health 1378.
Ivask, A., Titma, T., Visnapuu, M., Vija, H., Kakinen, A., Sihtmae, M., Pokhrel, S., Madler, L., Heinlaan, M., Kisand, V., Shimmo, R., Kahru, A., 2015. Toxicity of 11 metal oxide nanoparticles to three mammalian cell types in vitro. Curr. Top. Med. Chem. 15 (18), 1914–1929.
Kalia, S., Dufresne, A., Cherian, B.M., Kaith, B.S., Averous, L., Njuguna, J., Nassiopoulos, E., 2011. Cellulose-based bio- and nanocomposites: a review. Int. J. Polym. Sci. 201135.
Kisin, E.R., Murray, A.R., Sargent, L., Lowry, D., Chirila, M., Siegrist, K.J., Schwegler-Berry, D., Leonard, S., Castranova, V., Fadeel, B., Kagan, V.E., Shvedova, A.A., 2011. Genotoxicity of carbon nanofibers: are they potentially more or less dangerous than carbon nanotubes or asbestos? Toxicol. Appl. Pharmacol. 252 (1), 1–10.
Knudsen, K.B., Kofoed, C., Espersen, R., Hojgaard, C., Winther, J.R., Willemoes, M., Wedin, I., Nuopponen, M., Vilske, S., Aimonen, K., Weydahl, I.E., Alenius, H., Norppa, H., Wolff, H., Wallin, H., Vogel, U., 2015. Visualization of nanofibrillar cellulose in biological tissues using a biotinylated carbohydrate binding module of beta-1,4-glycanase. Chem. Res. Toxicol. 28 (8), 1627–1635.
Kogiso, M., Nishiyama, A., Shinohara, T., Nakamura, M., Mizoguchi, E., Misawa, Y., Guinet, E., Nouri-Shirazi, M., Dorey, C.K., Henriksen, R.A., Shibata, Y., 2011. Chitin particles induce size-dependent but carbohydrate-independent innate eosinophilia. J. Leukoc. Biol. 90 (1), 167–176.
Landsiedel, R., Fabian, E., Ma-Hock, L., van Ravenzwaay, B., Wohlleben, W., Wiench, K., Oesch, F., 2012. Toxico-/biokinetics of nanomaterials. Arch. Toxicol. 86 (7), 1021–1060.
Moon, R.J., Martini, A., Nairn, J., Simonsen, J., Youngblood, J., 2011. Cellulose nanomaterials review: structure, properties and nanocomposites. Chem. Soc. Rev. 40 (7), 3941–3994.
Murray, A.R., Kisin, E.R., Tkach, A.V., Yanamala, N., Mercer, R., Young, S.H., Fadeel, B., Kagan, V.E., Shvedova, A.A., 2012. Factoring-in agglomeration of carbon nanotubes and nanofibers for better prediction of their toxicity versus asbestos. Part Fibre Toxicol. 910.
Ni, H., Zeng, S., Wu, J., Cheng, X., Luo, T., Wang, W., Zeng, W., Chen, Y., 2012. Cellulose nanowhiskers: preparation, characterization and cytotoxicity evaluation. Biomed. Mater Eng. 22 (1–3), 121–127.
NIOSH, 2010. Current Intelligence Bulletin: Occupational Exposure to Carbon Nanotubes and Nanofibers. U.S. Department of Health and Human Services, Public Health Service, Centers for Disease Control, National Institute for Occupational Safety and Health, Cincinnati, OH. DHHS (NIOSH) Docket Number: NIOSH 161-A; Available at: http://www.cdc.gov/niosh/docket/review/docket161A/.
Österberg, M., Cranston, E.D., 2014. Special issue on nanocellulose. Nordic Pulp Pap. Res. J. 29 (1) eci.
Pascual, R.M., Peters, S.P., 2005. Airway remodeling contributes to the progressive loss of lung function in asthma: an overview. J. Allergy Clin. Immunol. 116 (3), 477–486 quiz 487.
Peng, B.L., Dhar, N., Liu, H.L., Tam, K.C., 2011. Chemistry and applications of nanocrystalline cellulose and its derivatives: a nanotechnology perspective. Can. J. Chem. Eng. 89 (5), 1191–1206.
Peng, Y., Gardner, D.J., Han, Y., Kiziltas, A., Cai, Z., Tshabalala, M.A., 2013. Influence of drying method on the material properties of nanocellulose I: thermostability and crystallinity. Cellulose 20 (5), 2379–2392.
Pereira, M.M., Raposo, N.R., Brayner, R., Teixeira, E.M., Oliveira, V., Quintao, C.C., Camargo, L.S., Mattoso, L.H., Brandao, H.M., 2013. Cytotoxicity and expression of genes involved in the cellular stress response and apoptosis in mammalian fibroblast exposed to cotton cellulose nanofibers. Nanotechnology 24 (7), 075103.
Perkel, J.M., 2012. Life science technologies: animal-free toxicology: sometimes, in vitro is better. Science 335 (6072), 1122–1125.
RCoreTeam, 2014. R: A Language and Environment for Statistical Computing from. http://www.R-project.org/.
Reese, T.A., Liang, H.E., Tager, A.M., Luster, A.D., Van Rooijen, N., Voehringer, D., Locksley, R.M., 2007. Chitin induces accumulation in tissue of innate immune cells associated with allergy. Nature 447 (7140), 92–96.
Roman, M., 2015. Toxicity of cellulose nanocrystals: a review. Ind. Biotechnol. 11 (1), 25–33.
Roy, R.M., Wuthrich, M., Klein, B.S., 2012. Chitin elicits CCL2 from airway epithelial cells and induces CCR2-dependent innate allergic inflammation in the lung. J. Immunol. 189 (5), 2545–2552.
Sayes, C.M., Reed, K.L., Warheit, D.B., 2007. Assessing toxicity of fine and nanoparticles: comparing in vitro measurements to in vivo pulmonary toxicity profiles. Toxicol. Sci. 97 (1), 163–180.
Shvedova, A.A., Yanamala, N., Kisin, E.R., Tkach, A.V., Murray, A.R., Hubbs, A., Chirila, M.M., Keohavong, P., Sycheva, L.P., Kagan, V.E., Castranova, V., 2014. Long-term effects of carbon containing engineered nanomaterials and asbestos in the lung: one year postexposure comparisons. Am. J. Physiol. Lung Cell Mol. Physiol. 306 (2), L170–L182.
Shvedova, A.A., Kisin, E.R., Yanamala, N., Farcas, M.T., Menas, A.L., Williams, A., Fournier, P.M., Reynolds, J.S., Gutkin, D.W., Star, A., Reiner, R.S., Halappanavar, S., Kagan, V.E., 2016. Gender differences in murine pulmonary responses elicited by cellulose nanocrystals. Part Fibre Toxicol. 13 (1), 28.
Van Dyken, S.J., Garcia, D., Porter, P., Huang, X., Quinlan, P.J., Blanc, P.D., Corry, D.B., Locksley, R.M., 2011. Fungal chitin from asthma-associated home environments induces eosinophilic lung infiltration. J. Immunol. 187 (5), 2261–2267.
Yanamala, N., Farcas, M.T., Hatfield, M.K., Kisin, E.R., Kagan, V.E., Geraci, C.L., Shvedova, A.A., 2014. In vivo evaluation of the pulmonary toxicity of cellulose nanocrystals: a renewable and sustainable nanomaterial of the future. ACS Sustain Chem. Eng. 2 (7), 1691–1698.